Progressive-Resolution Transmission and Lossless Compression of Color Images for Digital Image Libraries

Norbert Strobel, Sanjit K. Mitra, and B.S. Manjunath

Image Processing Laboratory
Department of Electrical and Computer Engineering
University of California, Santa Barbara 93106
Telephone: (805) 893-8312

Email: strobel@iplab.ece.ucsb.edu

Abstract— **Progressive-resolution transmission is of significant practical importance for online image libraries. When combined with reversible image compression, it provides a particularly promising framework which not only contributes to lower storage overhead but also to smaller transmission costs.**

We propose an efficient lossless compression scheme for RGB color images. It consists of a modified reversible subband transformation which is followed by a reversible color decorrelation technique. Switching the (traditional) order of wavelet and spectral transform offers the opportunity to support progressive–resolution transmission of spectrally decorrelated wavelet coefficients without compromising compression performance.

I. Introduction

With advances in storage, processing, and communications technologies, the creation of large digital image collections has become a practical reality. Applications of such image libraries can be found in many areas where they provide picture support for spatially referenced data sets [1], or improve the accessibility of large photograph collections [2].

Image databases are often designed for applications where images are archived for future processing or analysis. In these cases lossy compression methods are often objected to as users fear the irreversible loss of information. Some of the most effective methods for reversible compression involve linear predictive coding [3]. This form of compression is usually defined for a single resolution and the image can only be recovered in its entirety. On the other hand, a multiresolution approach based on progressive resolution transmission is more suitable for interactive exploration and browsing of digital image databases. Among several reversible multiresolution representations, the S-transform [4], the RTS-transform [5], and the S+P-transform [6] are particularly well suited for image database applications. In this paper a modified reversible wavelet transform is introduced first. Even though it is generally accepted that monochrome wavelet techniques can be used to separately compress image bands, such an approach fails to take into account potential correlations present between bands. As a result, a reversible color decorrelation technique is added next to exploit spectral redundancy.

This paper is organized as follows: In Section II, we revisit the reversible (intraband) wavelet transform. The description of a new spectral decorrelation technique follows in Section III. In Section IV, computer simulations are provided to demonstrate that switching the order of wavelet and spectral transform offers the opportunity to support progressive resolution image reconstruction without compromising compression performance. Finally, Section V discusses our results and offers some conclusions.

This work was funded in part by NSF grant IR194–11330, and by a University of California MICRO grant with matching support from the Xerox Corporation.

II. Reversible Wavelet Transform

One important difference between lossy and reversible compression is that the latter must not discard any information while the former can greatly benefit from such a strategy to improve its compression efficiency. In other words, while lossy compression provides the freedom to quantize transform coefficients to some smaller set, a good reversible image transform must limit the maximum number of bits required to represent each pixel in the transformed image.

The S–transform, which is similar to the Haar transform [7] reduces the necessary data precision by making intelligent use of rounding operations. It transforms an input image $x_0[m,n], m = 0,\ldots,M-1, n = 0,\ldots,N-1$, with M and N even, into four

0–7803–4137–6/97/$10.00©1977 IEEE

subbands denoted by LL, LH, HL, and HH. Since the original image lies at the bottom of a pyramid decomposition, it carries the index zero. Due to truncation, the maximum number of bits required to represent the LL-band, composed of local averages, does not change. The detail signals, which comprise positive and negative integers require more bits.

The rounding operations introduce a nonlinearity into the S-transform which produces a noteworthy side-effect. Since usually only truncation operations are used, fractional parts are always discarded. As a result, the transform becomes biased, i.e., local means as computed by the S-transform are on the average smaller than those obtained without truncation. A simple solution to this problem can be found by realizing that the S-transform is only one (separable) example of a whole family of rounding transforms. To balance the roundoff error one can apply a rounding up operation along the image rows while using the truncation operation along the columns.

As shown in Eq. (1), we obtain a *balanced* S-transform by truncating averaged column means. The local column averages are computed according to Eq. (2) where a rounding up operation is applied to the mean of neighboring row pixels. More precisely, LL pixels $x_{k+1}[m,n]$ at successive decomposition levels $k+1$ are obtained as

$$x_{k+1}[m,n] = \lfloor \frac{\bar{x}_k[2m] + \bar{x}_k[2m+1]}{2} \rfloor, \qquad (1)$$

where the (rounded up) averages $\bar{x}_k[r]$ at row r and level k are computed via

$$\bar{x}_k[r] = \lceil \frac{x_k[r,2n] + x_k[r,2n+1]}{2} \rceil. \qquad (2)$$

The balanced S-transform alternates between opposite rounding operations along the rows and columns and achieves an unbiased ("balanced") roundoff error while the remaining LH, HL and HH subbands (wavelet coefficients) are computed in the traditional (separable) way. The balanced S-transform yields lowpass coefficients which can be modeled by a sum of (true) local mean and additive, zero mean noise.

The weakness of the (balanced) S-transform is the comparatively large entropy and energy of the detail (or wavelet) coefficients when compared to other subband transforms. However, an interband prediction method independently proposed by Said [6] and Kuroki [9] can be used to significantly improve decorrelation between detail coefficients, thus improving coding efficiency.

Interband prediction, as explained for the 1-D case and shown in Fig. 1, uses the derivative of the lowband coefficients at decomposition level k, denoted by $\Delta x_k[n]$, where

$$\Delta x_k[n] = x_k[n-1] - x_k[n], \qquad (3)$$

to predict the high-band (or wavelet) coefficients $d_k[n]$ via

$$\hat{d}_k[n] = \sum_{i=-L_0}^{L_1} \alpha_i \, \Delta x_k[n+i]. \qquad (4)$$

Finally the prediction difference $\tilde{d}_k[n]$ is formed by subtracting rounded predictor outputs from the high-band coefficients:

$$\tilde{d}_k[n] = d_k[n] - [\hat{d}_k[n]] \qquad (5)$$

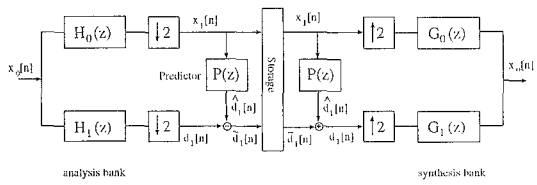

Fig. 1. Interband prediction in 1-D: The predictor $P(z)$ is used to predict detail signals $d_1[n]$ at, e.g., decomposition level 1 from differences between associated approximation coefficients $x_1[n]$.

If we ignore rounding operations and interchange (linear) predictors $P(z)$ with down-samplers/up-samplers, then interband prediction can be explained in terms of an *equivalent* filter bank. Here the equivalent analysis highpass filter $\tilde{H}_1(z)$, given by

$$\tilde{H}_1(z) = H_1(z) - P(z^2)H_0(z) \qquad (6)$$

replaces the original highpass filter $H_1(z)$, and the equivalent synthesis lowpass filter $\tilde{G}_0(z)$, defined as

$$\tilde{G}_0(z) = G_0(z) + P(z^2)G_1(z) \qquad (7)$$

substitutes for its original counterpart $G_0(z)$. While $\tilde{H}_1(z)$ can now be designed to better decorrelate input signals, care must be taken to ensure that the synthesis lowpass filter $\tilde{G}_0(z)$ still interpolates well. With $H_0(z)$ and $H_1(z)$ taken to be S-transform filters, the equivalent analysis highpass filter $\tilde{H}_1(z)$ is given by

$$\tilde{H}_1(z) = (z-1)[\frac{(z^{-1}+1)^2}{2} \sum_{i=-L_0}^{L_1} \alpha_i z^{+2i} - 1]. \qquad (8)$$

Similarly the equivalent synthesis lowpass $\tilde{G}_0(z)$ follows as

$$\tilde{G}_0(z) = (z^{-1}+1)[1 - \frac{(z^{-1}-1)^2}{2} \sum_{i=-L_0}^{L_1} \alpha_i z^{+2i}]. \qquad (9)$$

Choosing $\alpha_0 = \alpha_1 = \frac{1}{4}$, for example, results in the RTS transform. This prediction idea also connects to average-interpolation as introduced by Donoho [10].

III. Reversible Color Transforms

When compressing images with spectrally correlated components, color conversion can be very beneficial. Traditional transformations from the RGB domain to, e.g., the YUV or YIQ space are, however, often irreversible when arithmetic precision is limited.

Recently a lossless color transform has been proposed which takes N bit RGB components and produces an N-bit Yr component and N+1 bit Ur and Vr channels [12]. These can be thought of as (reversible) approximations of YUV color components [13]. Although for most images investigated an improvement of over 10% was reported, the color transform suggested cannot be directly applied to lossless progressive–resolution transmission. In other words, since a (nonlinear) spectral transform is followed by a (nonlinear) spatial transform, the latter processing step has to be reversed first before the inverse color transformation can be taken. Therefore, lossless progressive–resolution transmission cannot be directly supported since the inverse color transformation can only be taken at the final resolution.

As a result, a modified color compression scheme is needed if progressive–resolution transmission is to benefit from additional spectral decorrelation. We propose a new method shown in Fig. 2 where the traditional order of interband and intraband transform has been interchanged. A reversible wavelet transform is used to first (intraband) decorrelate the red, green, and blue color bands before an (interband) rounding transform is applied to the color components of each subband.

More precisely, let $\mathbf{y}[m,n]$ be a vector of subband coefficients comprising the red, green, and blue (integer) transform coefficients $r[m,n]$, $g[m,n]$, and $b[m,n]$, at spatial location $[m,n]$:

$$\mathbf{y}[m,n] = [r[m,n]\, g[m,n]\, b[m,n]]^t. \tag{10}$$

Then the forward (color) rounding transform of an (integer) vector $\mathbf{y}[m,n]$ can be defined as

$$\mathbf{z}[m,n] = \left\lceil \mathbf{R}\,\mathbf{y}[m,n] \right\rceil, \tag{11}$$

while its inverse transform is given by

$$\mathbf{y}[m,n] = \left\lfloor \mathbf{R}^{-1}\,\mathbf{z}[m,n] \right\rfloor. \tag{12}$$

Here $\lceil . \rceil$ and $\lfloor . \rfloor$ denote rounding up and rounding down operations which take the nearest larger integer value and the nearest smaller one, respectively.

A sufficient condition for the transform to be reversible is that the non-singular *rounding* matrix $\mathbf{R}$ has the following properties [8]:

1. All its elements are integers except in the first row where they have to add up to one.
2. The sum of all (integer) elements in each of the other rows has to be zero.

We chose the following $\mathbf{R}$ such that our results can be directly compared to those presented in [12]:

$$\mathbf{R} = \begin{bmatrix} 0.25 & 0.50 & 0.25 \\ 1 & -1 & 0 \\ 0 & -1 & 1 \end{bmatrix} \tag{13}$$

Although the spectral transforms are formulated slightly differently, a close look reveals that both are equivalent. At this stage the main difference between both methods is the order of wavelet and color transforms.

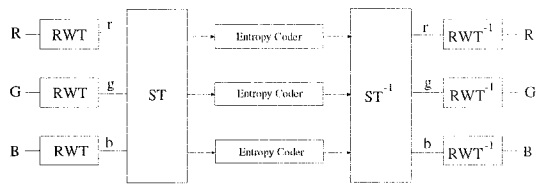

Fig. 2. Multiresolution color transform scheme: A reversible (intraband) wavelet (or subband) transform (RWT) is performed first. It is followed by a spectral (interband) transform (ST) further decorrelating subband coefficients along the spectral dimension. Finally all spectral components of the color–transformed subbands can be entropy encoded individually.

IV. Experimental Results

In this section we follow the classical approach to lossless compression where spatial decorrelation is performed first and entropy coding of the decorrelated signals is applied next. Two different reversible transforms are investigated. They consist of separable reversible 2-D wavelet transforms taken over six levels which are followed by integer spectral transforms (ST). The two transforms employ the same spectral decorrelation method but differ in the prediction schemes used. They are specified as:

- RWT 1: $\alpha_i = 0$, $\forall i$ (balanced S transform.)
- RWT 2: $\alpha_0 = \alpha_1 = 1/4$ (RTS transform.)

The compression performance is assessed by measuring the total zeroth-order entropy H_{tot}. It is calculated over all spectral components (u,v,w) of subbands at all decomposition levels $k \in \{1, \ldots, L\}$. Subbands carry two subscripts k and s. The former denotes the decomposition level, while later indicates the spectral component. Since individual subband entropies contribute to H_{tot} according to the relative size of their associated subbands, they are weighted accordingly:

$$
\begin{aligned}
H_{tot} &= \frac{1}{4^L} \sum_{s\in\{u,v,w\}} H(LL_{L,s}) \\
&+ \sum_{k=1}^{L} \frac{1}{4^k} \{ \sum_{s\in\{u,v,w\}} H(LH_{k,s}) \\
&+ \sum_{s\in\{u,v,w\}} H(HL_{k,s}) \\
&+ \sum_{s\in\{u,v,w\}} H(HH_{k,s}) \}.
\end{aligned}
\tag{14}
$$

Table I shows the results obtained for a set of six different test images. The second (fourth) table column contains entropies (in bits/coefficient) obtained using the RWT 1 (RWT 2) without any subsequent spectral transform. Column three (five) provides results when RWT 1 (RWT 2) is followed by the spectral transform specified in Eq. (13).

TABLE I
ENTROPY COMPARISON

	RWT 1		RWT 2	
Images	no ST	with ST	no ST	with ST
barb	16.59	10.29	15.46	12.37
boats	14.23	8.95	13.50	11.00
fruits	8.65	9.01	9.15	9.41
girl	14.13	9.13	13.02	11.16
zelda	13.25	8.54	12.44	10.60
gold	15.25	9.85	14.73	12.43

V. Discussion and Conclusions

Several observations can be made: First, without any spectral transform RWT 2 generally outperforms RWT 1. This could be expected since RWT 2 is based on a better highpass filter. However, the results change with the application of the spectral transform. Now RWT 1 yields significantly lower entropies than RWT 2. Although spectral decorrelation is usually beneficial to lower the entropy of color pictures, the same cannot be said for the "fruits" image. There a statistical analysis reveals little correlation between color components which explains why the spectral transform is counter productive.

A statistical analysis, furthermore, shows that RWT 1's short, two-tap highpass filter generates subband color coefficients which are more strongly cross correlated across different color bands than in the case of RWT 2. It is exactly this cross correlation which the subsequent spectral transform can greatly benefit from. Note, however, that even after the spectral transform, the resulting subband color components are not completely uncorrelated.

We presented a reversible multiresolution transform for the progressive–resolution transmission of intraband and interband transformed color images. Experimental results indicate that our approach offers a remarkable decorrelation potential given its low computational complexity. Further work is necessary to evaluate how well our approach performs when an entropy coder is added.

References

[1] T. Smith *et al.*, "A digital library for geographically referenced materials," *IEEE Computer Magazine*, vol. 29, pp. 54–60, May 1996.

[2] V. E. Ogle and M. Stonebraker, "Chabot: Retrieval from a relational database of images," *IEEE Computer Magazine*, vol. 28, pp. 40 – 48, September 1995.

[3] G. R. Kuduvalli and R. M. Rangayyan, "Performance analysis of reversible image compression techniques for high-resolution digital teleradiology," *IEEE Trans. Med. Imaging*, vol. 11, pp. 430–445, 1992.

[4] T. H. Wendler and D. Meyer-Ebrecht, "Proposed standard for variable format picture processing and a codec approach to match diverse imaging devices," in *Proceedings of the SPIE*, vol. 318, pp. 298–305, 1982.

[5] A. Zandi, J. Allen, E. Schwartz, and M. Boliek, "CREW: compression with reversible embedded wavelets," in *Proc. IEEE Data Compression Conference*, (Snowbird, Utah), pp. 212–221, March 1995.

[6] A. Said and W. A. Pearlman, "An image multiresolution representation for lossless and lossy compression," *IEEE Transactions on Image Processing*, vol. 5, pp. 1303–1310, 1996.

[7] M. Vetterli and J. Kovacevic, *Wavelets and Subband Coding*. Englewood Cliffs, NJ: Prentice Hall, 1995.

[8] H. Y. Jung, T. Y. Choi, and R. Prost, "Rounding transforms for lossless image coding," in *Proc. ICIP 1996*, pp. 65–68, 1996.

[9] N. Kuroki and M. Numa, "Haar wavelet transform with interband prediction and its application to image coding," *Electronics and Communications in Japan, Part 3*, vol. 78, no. 4, pp. 1738–1746, 1995.

[10] D. Donoho, "Smooth wavelet decompositions with blocky coefficient kernels," in *Recent Advances in Wavelet Analysis* (L. Schumaker and G. Webb, eds.), New York, Academic Press, 1993.

[11] A. Cohen, I. Daubechies, and J. Feauveau, "Biorthogonal bases of compactly supported wavelets," *Comm. Pure Appl. Math.*, no. 45, pp. 485–560, 1992.

[12] M. J. Gormish, E. Schwartz, A. Keith, M. Boliek, and A. Zandi, "Lossless and nearly lossless compression for high quality images," in *Proceedings of the SPIE*, vol. 3025, (San Jose, CA), February 1997.

[13] CCIR, "Recommendation 601-1, Encoding Parameters of Digital Television for Studios," Question 25/11, Study Programmes 25G/11, 25H/11, CCIR, 1982-86.